# Finite Element Analysis of Hypar Shell footing on Elastic Foundation

Rafa'a M. Abbas
*Civil Engineering Department, College of Engineering, University of Baghdad*

Ali A. Abdulhameed
*Department of Engineering Affairs, University of Baghdad /Baghdad*

Ali I. Salahaldin
*Civil Engineering Department, College of Engineering, University of Baghdad*

ABSTRACT: In this research the performance of the hyperbolic paraboloid shell foundation is investigated. The two components of the interacting system; the soil and the shell foundation are modeled using finite element via developed finite element analysis computer programme. The foundation shell is modeled using degenerated layered shell elements, while the soil-structure interaction between the shell elements and the supporting medium are modeled by representing the soil by certain analytical equivalent such as Winkler model with both normal compressional and tangential frictional resistances.

Finite element analysis results from the present study are compared with published results and with the numerical results of three-dimensional finite element model using finite element code, ANSYS. Comparison reveals that present study results compare well with other analytical and numerical results.

Parametric study has been carried out to investigate the effect of some important parameters on the behaviour of the hyper foundations such as shell thickness, shell warp, ridge and edge beams stiffness. The study shows that shell maximum settlement is reduced by 40% with the increase of shell warp from 0.08 to 0.40 $m^{-1}$, and reduced by 19% when shell thickness is increased from 150 to 300mm. As a result, load carrying capacity is increased with increasing shell warp and thickness.

## 1 INTRODUCTION

Although shells have been enjoying wide and varied use in roofs, they are new comers to the family of structural foundations. It is about five decades only since Felix Candela in 1953 poured his first hypar shell footing on the Mexican soil. Whatever may appear strange is the fact that the concept of shells is not new in foundations, if one would consider the old inverted arch foundations as belonging to this group. The use of brick arches in foundations has been in practice for a long time in many countries.

The twin attributes of a shell that recommend its use in roofs are economy and aesthetics. Since the latter aspect is of no concern in a buried structure like the foundation, here, the aspect of economy which holds the key to the acceptance and use of shells in foundations. Foundation shells differ from roof shells in the following important respects, Kurian (1982):

- Shells used in foundations are invariably characterized by small sizes and greater thickness as compared to those used in roofs.
- The self-weight of the foundation shell is directly transmitted to the soil, and thus no significant stresses are induced in the shell on account of this weight, unlike in roofs, where the self-weight may constitute the major part of the loading.

- Since foundation shells bear directly on soil at their bottom and carry backfill on top, besides being thick, the problem of buckling is of lesser concern in foundation shells.

There are some common types of shells which are frequently used in foundations. Among the shells, which have come into wider use, the hyperbolic paraboloid (or briefly hypar) shell has been the most important type (Figure 1a). Besides its geometric simplicity, resulting from its straight-lines property, the hypar shell has high structural efficiency. The hypar shell lends itself for effective use not only as individual footings, but also as combined footings for columns.

The frustum of a cone is probably the simplest form in which a shell can be put to use in foundations. While smaller shells of this type can be used as footings for columns (Fiure 2b), shells of larger dimensions can serve as rafts for tower-shaped structures such as chimneys.

Sectors of spherical shells in the inverted position with ring beam (Figure 3c) have been used as feasible foundations for cylindrical structures such as water tanks supported on a circular row of columns, in place of heavily reinforced flat circular rafts of substantial thickness.

Folded plates of various shapes can be used as foundations as shown in Figure 4d. This type of folded plate foundation can be used as individual footing or can be combined to serve as combined footings or rafts.

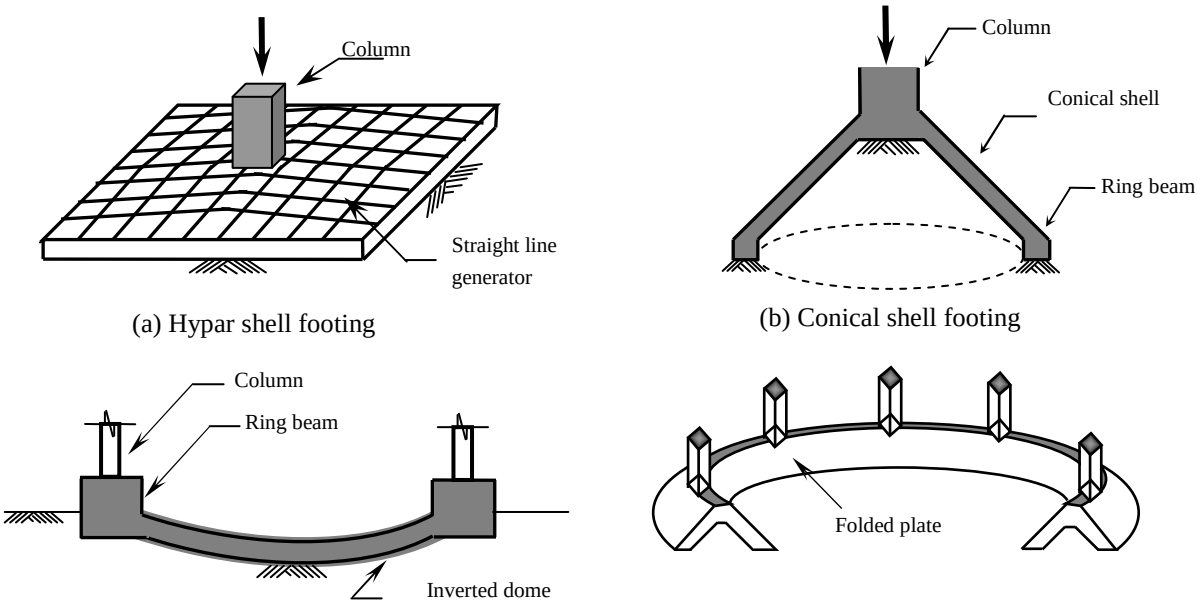


(a) Hypar shell footing

(b) Conical shell footing

(c) Spherical shell footing

(d) Folded plate footing

Figure1. Typical types of shell footing

Many theoretical studies have reported the structural behavior of shell foundations. Some studies utilized the finite difference for the elastic solution of hypar shell (Melerski, 1986). While the early attempt to analze shell foundation using the finite element method available in literature seems to be by Jain,Nayak and Jain (1977). Many other studies (Bairagi and Buragohain, 1985; Maharaj, 2003; Huat and Mohammed, 2006) have utilized the finite element method for the analysis of different shell foundations.

In some studies the soil-structure interaction between shell footing and supporting soil was simulated using Winkler soil model. Kurian (1977) developed a flexural analysis resulting from a series of solutions for a hyperbolic paraboloid shell with simply supported edges resting on a Winkler subgrade. In other paper, Kurian (1993) investigated the effect of subgrade reaction on hypar and conical shells. Finite element method simulating the soil as Winkler model was utilized by Kurian (1994 ,1995). All studies reached the same conclution concerning the increase of load carrying capacity with increasing soil modulus.

Ramiah *et al* (1977) carried out experimental studies on a grid square hyperbolic paraboloid shell footing. Bearing test were conducted on shells and plates on the surface of dry sand to

evaluate the ultimate bearing capacity and settlements. Huat *et al* (2007) investigated experimentally and theoretically the performance of triangular shell footing. A parametric study was carried to examine the effect of some parametres on shell load carrying capacity.

This paper describes a study on the geotechnical performance of the hypar shell footing using finite element method in which the soil is represented using linear Winkler model with both normal compressional and tangential resistances. A parametric study is carried out to examine the effect of different parameters on the behaviour of such footings.

## 2 IDEALIZED MODEL FOR ELASTIC FOUNDATION

Contact pressures are the reactive pressures offered by the soil onto the foundation, at the interface between the foundation and the soil, against the loads transmitted to the soil through the foundations. Theoretically, the contact pressure developing at the interface between the foundation and soil has two components; normal and tangential.

Several investigators have used the theory of elasticity to solve soil-structure interaction problems. The soil is treated as a semi-infinite, homogeneous, isotropic and elastic material. Results by this approach are not completely correct except for special cases. In general, the soil medium will exert both compressional (or normal) and frictional (or tangential) resistances. There are several suggested models for the two response components of soil.

### 2.1 *Compressional resistance model*

The compressional resistance is the transverse reaction of the soil medium to the overlying footing, Scott (1981). Winkler model is used in the present study to simulate the compressional (normal) resistance. Winkler's model assumes that the base is consisting of closely spaced independent linear springs; consequently, the contact pressure at any point on the soil-structure contact is proportional to the deflection at that point and is independent of deflection at the others. This model is a one-parameter model. The pressure *P(x,y)* beneath the foundation is given by:

$$P(x, y) = K_z \cdot w(x, y) \tag{1}$$

Where, $K_z$ is the modulus of subgrade reaction and *w* is the deflection in the *z* direction.

### 2.2 *Frictional resistance model*

The applied loads on shell resting on an elastic foundation produce deformation in the contact face of the shell with soil. These movements cause shearing (or friction) force at the shell-foundation interface. The magnitude of the frictional force is dependent on the soil, shell and on the applied loads. These shearing forces produce distributed moments and membrane forces in the foundation shell.

There are many assumptions for the interface condition between a foundation and underlying soil medium. These range from the completely smooth to the completely adhering interface. The frictional resistance to the tangential movement is either Winkler friction, Coulomb friction, constant friction or Newton friction.

According to the definition of compressional Winkler model, the frictional resistance could be:

$$F_x(x, y) = K_x \cdot u(x, y)_{(z=-h/2)}$$

$$F_y(x, y) = K_y \cdot v(x, y)_{(z=-h/2)} \tag{2}$$

where $F_x$ and $F_y$ are the frictional forces per unit area in the x and y directions, respectively, and $K_x$ and $K_y$ are the moduli of subgrade reaction in the x and y directions, respectively. $u(x,y)_{(z=-h/2)}$ and $v(x,y)_{(z=-h/2)}$ are the horizontal displacements in the x and y directions, respectively, as shown in

Figure 2. Equation (2) shows that the friction forces $F_x$ and $F_y$ varies linearly with the horizontal displacements $u(x,y)_{(z=-h/2)}$ and $v(x,y)_{(z=-h/2)}$, respectively.

Moments $M_x$ and $M_y$ (per unit width) in the x and y Cartesian coordinates directions are developed due to the frictional forces existence $F_x$ and $F_y$ (per unit width) in the xz and yz plane, respectively, and they are:

$$M_x = \frac{h}{2} \cdot F_x \qquad \text{and} \qquad M_y = \frac{h}{2} \cdot F_y \tag{3}$$

or

$$M_x = \frac{h}{2} \cdot K_x \cdot u_{(z=-h/2)} \qquad \text{and} \qquad M_y = \frac{h}{2} \cdot K_y \cdot v_{(z=-h/2)} \tag{4}$$

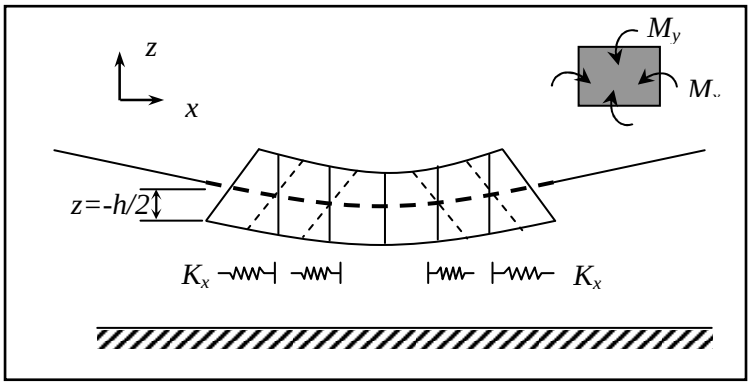


Figure 2. Winkler frictional model

## 3 FINITE ELEMENT FORMULATION

In this research the shell foundation and the supporting soil medium are modeled and analyzed via a developed finite element computer programme.

For the hyperbolic paraboloid shell, 9-node isoparametric degenerated shell element with five degrees of freedom at each node are used. Soil-structure interaction between the shell elements and the supporting medium are modeled using Winkler model with both normal (compressional) and tangential (frictional) resistances.

For a foundation represented by Winkler model with both compressional and frictional resistances, the stiffness matrix is given by, Scott (1981):

$$[K]_f = \begin{bmatrix} [R_w] & 0 & .. & 0 \\ 0 & [R_w] & .. & 0 \\ .. & .. & .. & .. \\ 0 & 0 & .. & [R_w] \end{bmatrix}_{n \times n} \tag{5}$$

where n is the total number of nodes per element, and $[R_w]$ is defined as:

$$[R_w] = \begin{bmatrix} K_{f1} & 0 & 0 & 0 & 0 \\ 0 & K_{f2} & 0 & 0 & 0 \\ 0 & 0 & K_{f3} & 0 & 0 \\ 0 & 0 & 0 & K_{f4} & 0 \\ 0 & 0 & 0 & 0 & K_{f5} \end{bmatrix} \tag{6}$$

The stiffness of the foundation is distributed to the nodes of the element like the distribution of pressure load on the bottom surface of the element ($\zeta = -1$), thus at node k

$$K_{f1} = \int_{-1}^{+1}\int_{-1}^{+1} k_{x'} N^k(\xi,\eta)\left|J(\xi,\eta,\zeta)\right| d\xi \cdot d\eta$$

$$K_{f2} = \int_{-1}^{+1}\int_{-1}^{+1} k_{y'} N^k(\xi,\eta)\left|J(\xi,\eta,\zeta)\right| d\xi \cdot d\eta$$

$$K_{f3} = \int_{-1}^{+1}\int_{-1}^{+1} k_{z'} N^k(\xi,\eta)\left|J(\xi,\eta,\zeta)\right| d\xi \cdot d\eta \qquad (7)$$

$$K_{f4} = \int_{-1}^{+1}\int_{-1}^{+1} k_{x'} \frac{h_s^k}{2} N^k(\xi,\eta)\left|J(\xi,\eta,\zeta)\right| d\xi \cdot d\eta$$

$$K_{f5} = \int_{-1}^{+1}\int_{-1}^{+1} k_{y'} \frac{h_s^k}{2} N^k(\xi,\eta)\left|J(\xi,\eta,\zeta)\right| d\xi \cdot d\eta$$

where $K_{x'}$, $K_{y'}$ and $K_{z'}$ are the subgrade reaction coefficients in the local coordinates $x', y'$ and $z'$, $h_s^k$ is the thickness of the shell at node k, $N^k(\xi,\eta)$ is the shape function at node k and $\left|J(\xi,\eta,\zeta)\right|$ is the determinant of the Jacobian matrix.

The total stiffness of the shell-foundation system $[K]_{sf}$ will be:

$$[K]_{sf} = [K] + [K]_f \qquad (8)$$

The elastic foundation model is implemented in the finite element code, PLAST (Huang, 1989) and used in the present study.

## 4 FINITE ELEMENT MODEL VERIFICATION

Two hyperbolic paraboloid shell foundations are selected and modeled using the developed finite element programme. Results obtained from these models are compared with earlier published works. Also, the same shell foundations are analyzed using the available finite element software ANSYS to verify the adopted simple model with the three-dimensional model results.

The first hypar shell is a prototype shell foundation analyzed by Kurian (1993). Properties for the shell shown in Figure 3 are given in Table 1. Subgrade moduli are assumed to be $K_x = K_y = 0$, $K_z$ =50000, 100000, 200000 kN/m$^3$. Due to symmetry, one quadrant of the footing is analyzed. The quadrant is divided into nine 9-nodes isoparametric degenerated shell elements.

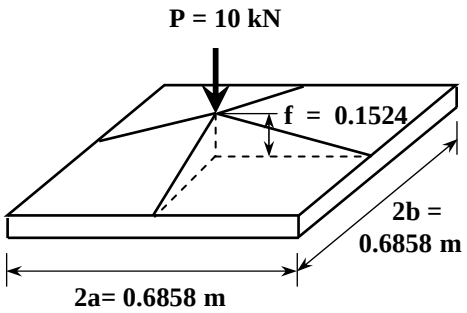


Figure3. Hypar shell model

Table 1: Hypar shell properties

| **Properties** | **Value** |
|---|---|
| Shell properties | |
| Column load ***(kN)*** | 10 |
| Thickness ***(m)*** | 0.00635 |
| Rise ***(m)*** | 0.1524 |
| Young's modulus ***(kN/m$^2$)*** | $75\times10^6$ |
| Poisson's ratio | 0.25 |
| Edge and ridge beam section ***(m×m)*** | 0.020×0.025 |

The same shell foundation was analyzed using finite element software ANSYS. The three dimensional brick elements, solid 45, with 3 dof per node was used to model soil medium. The hypar shell was modeled using shell elements, shell 43, with 6 dof per node, whereas edge and ridge beams were modeled using beam elements, beam 4, with 6 dof per node. ANSYS finite element model for one quadrant of the footing is shown in Figure 4.

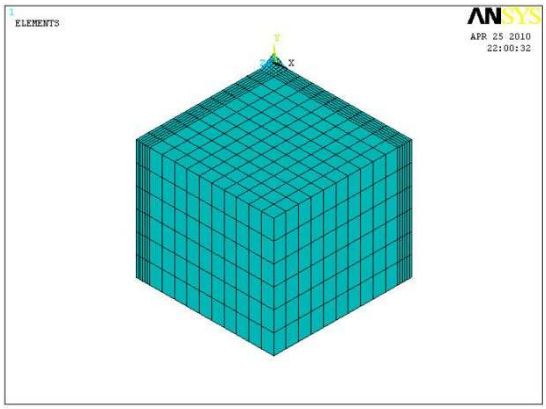


Figure4. ANSYS finite element model

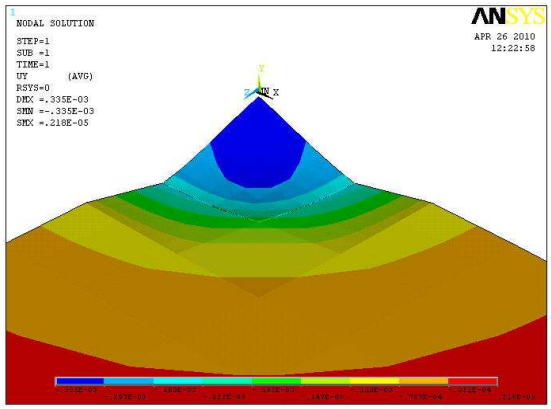


Figure5. Hypar shell deformation

Figure 6 shows the settlement curves for the hypar shell with different subgrade modulus values. Comparison between present study results and Kurian (1993) and ANSYS results is presented. In general there is a good agreement between present study and Kurian results. Also, ANSYS finite element results are slightly different from other results, however, they compare well with other results. Figure 5 shows the deformed ANSYS finite element model.

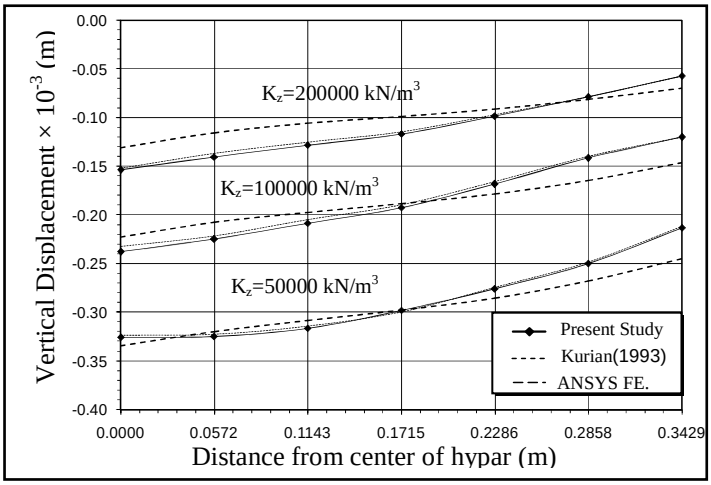


Figure 6. Vertical settlement along ridge beam

Melerski (1986) analyzed a square hypar shell footing by the finite difference method. Properties for the hypar shell with the same layout as in Figure 3 are given in Table 2. One quadrant of the shell was analyzed by the developed programme using 9-noded isoparametric shell elements. Also, the same shell foundation was analyzed using finite element software ANSYS. The hypar shell and the soil medium were discretized using 2295 different ANSYS finite elements as indicated for the first hypar shell analyzed previously.

Figure 7 shows the settlement curve for the hypar shell along the diagonal. Whereas, Figure 8 and 9 shows axial force variation in the edge and ridge beams, respectively. Comparison between present study results and Melerski (1986) and ANSYS results is presented. In general, different results compare well with each other.

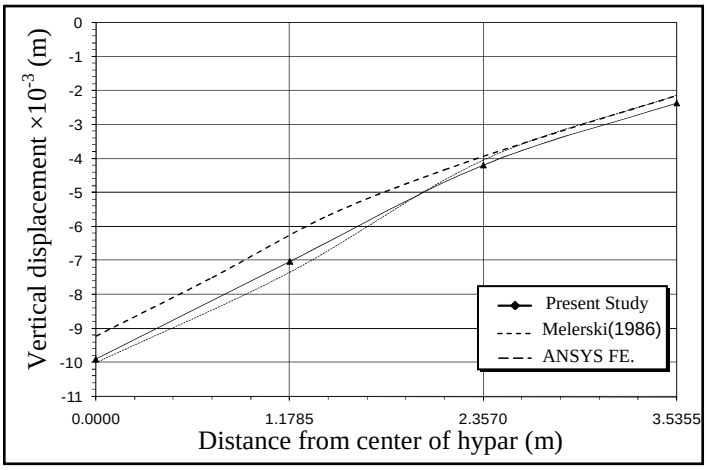


Figure 7. Vertical settlement along hypar diagonal

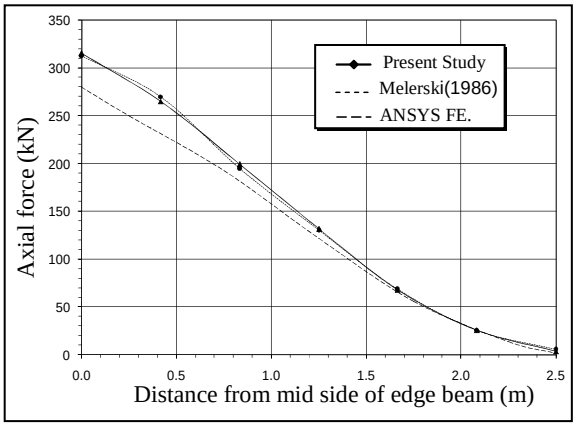


Figure 8. Axial force in the edge beam

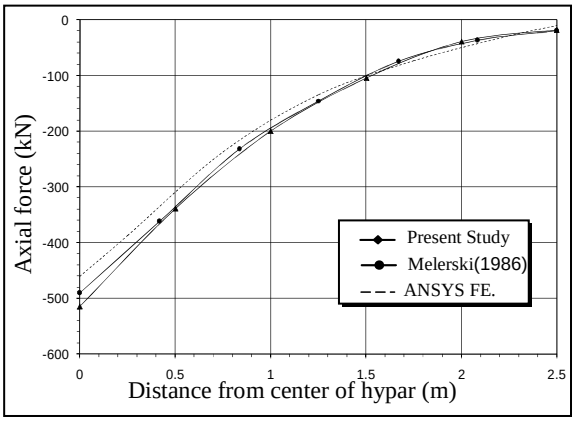


Figure 9. Axial force in the ridge beam

## 5 PARAMETRIC STUDY

In order to study the influence of selected parameters on the behaviour of the hypar shell foundations, a parametric study was carried out. Four parameters are considered which are: shell warp, shell thickness, ridge beam cross sectional dimensions and edge beam cross sectional dimensions.

The square hypar footing with the properties given in Table 2 was analyzed using the developed finite element computer programme. Comparison between the results of the different parameters is presented hereafter.

Table 2: Properties of the hypar shell footing

| **Properties** | **Value** |
|---|---|
| Shell properties | |
| Column load ***(kN)*** | 1600 |
| Size ***(m×m)*** | 5.0 × 5.0 |
| Thickness ***(m)*** | 0.10 |
| Rise ***(m)*** | 0.50 |
| Young's modulus ***($kN/m^2$)*** | $24\times10^6$ |
| Poisson's ratio | 0.0 |
| Edge and ridge beam section ***(m×m)*** | 0.20×0.30 |
| Foundation properties | |
| Modulus of subgrade reaction, $K_x=K_y=K_z$ ***($kN/m^3$)*** | 12000 |

5.1 *Shell warp*

The warp of the hypar shell is defined as:

$$k = f/ab$$

Where *f* is the shell rise and *a* and *b* are the plane dimensions of the hypar. Different values for the shell warp are taken (k = 0.08, 0.16, 0.24, 0.32, 0.4 $m^{-1}$).

Figure 10 shows the variation of the vertical displacement along the diagonal. This figure shows that as shell warp increases, shell deflection decreases at the centre and increases at the edge of the hypar. It is evident that plate action will governs shell behaviour with low rise (f) values, whereas as the warp of the shell increases the membrane action will govern the shell behaviour which produces more uniform settlement under shell.

This study shows that maximum settlement is reduced by 40% with the increase of shell warp from 0.08 to 0.40 $m^{-1}$, as a result, load carrying capacity is increased with increasing shell warp.

5.2 *Shell thickness*

Four values of shell thickness are considered in this study (h = 0.15, 0.2, 0.25 and 0.3m) to investigate the effect of this parameter.

Figure 11 shows the variation of the vertical displacement along the diagonal when shell thickness is increased from 0.15m to 0.30m. This figure indicates that as shell thickness increases, shell deflection decreases at the centre and increases along the edge of the hypar. It is obvious that shell rigidity increases as shell thickness increases and as a result more uniform settlement is produced under shell.

This study shows that maximum settlement is reduced by 19% with the increase of shell thickness from 0.15 to 0.30 m, as a result, load carrying capacity is increased with increasing shell thickness.

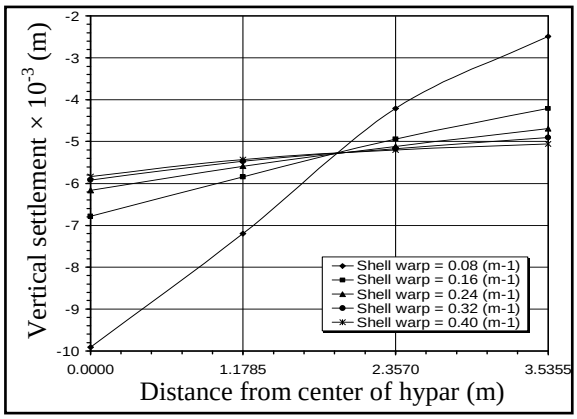


Figure 10: Effect of shell warp on shell vertical setllement

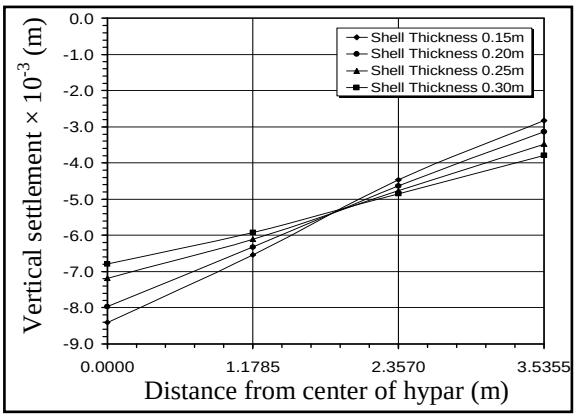


Figure 11: Effect of shell thickness on shell vertical setllement

5.3 *Ridge beam cross sectional dimensions*

Four values of ridge beam cross sectional dimensions are taken (0.20 m × 0.20 m, 0.20 m × 0.25 m, 0.20 m × 0.30 m and 0.20 m × 0.35 m) in this study.

Figure 12 shows the variation of the vertical displacement along the ridge beam.This figure shows that as ridge beam dimensions is increased, the vertical displacement at the center of the hypar shell will decrease due to increased stiffness of the shell footing.

Figures 13, 14 and 15 show the variation of the bending moment, shear force and axial force in the ridge beam, respectively. The values of the bending moment, shearing force and axial force in the ridge beam will increases with increasing its cross sectional dimensions. This behavior is due to the fact that as ridge beam stiffness is increased more forces will be tolerated by this beam.

5.4 *Edge beam cross sectional dimensions*

Four values of edge beam cross sectional dimensions are taken (0.20 m × 0.20 m, 0.20 m × 0.25 m, 0.20 m × 0.30 m and 0.20 m × 0.35 m) in this study.

Figure 16 shows the variation of the vertical displacement along the edge beam.This figure shows that as edge beam dimensions is increased, difference between mide side and corner settlement of the shell will decrease due to increased stiffness of the shell footing.

Figures 17, 18 and 19 show the variation of the bending moment, shear force and axial force in the ridge beam, respectively. The values of the bending moment, shearing force and axial force in the edge beam will increases with increasing its cross sectional area. This behavior is due to the fact that as edge beam stiffness is increased more forces will be tolerated by this beam.

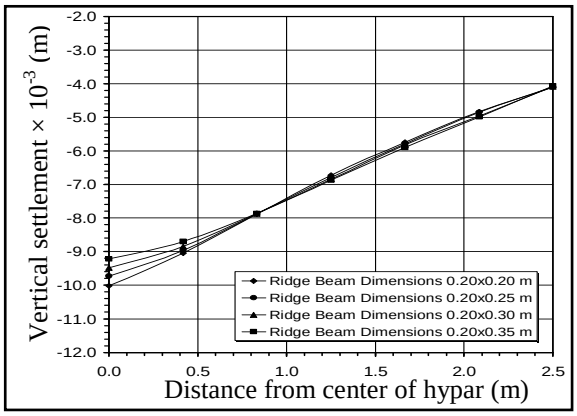


Figure 12: Effect of ridge beam on shell setllement

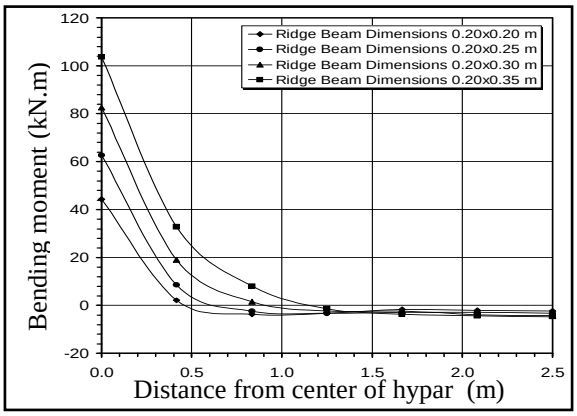


Figure 13: Ridge beam bending moment variation

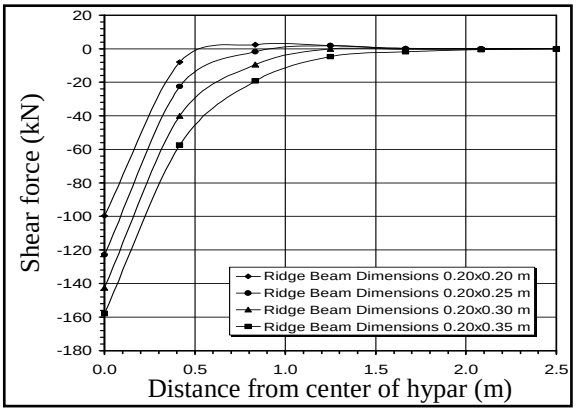


Figure 14: Ridge beam shear force variation

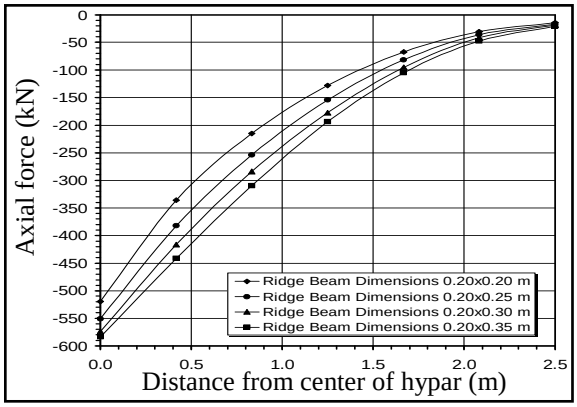


Figure 15: Ridge beam axial force variation

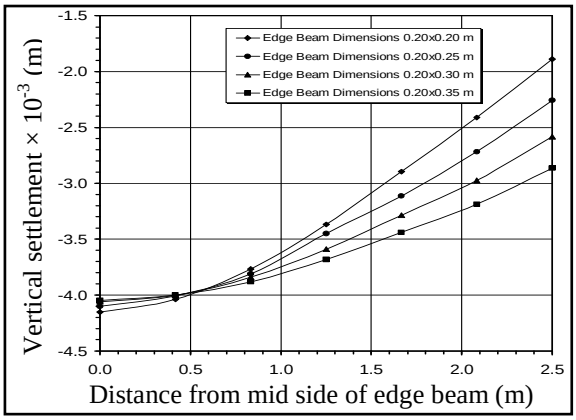


Figure 16: Effect of edge beam on shell setllement

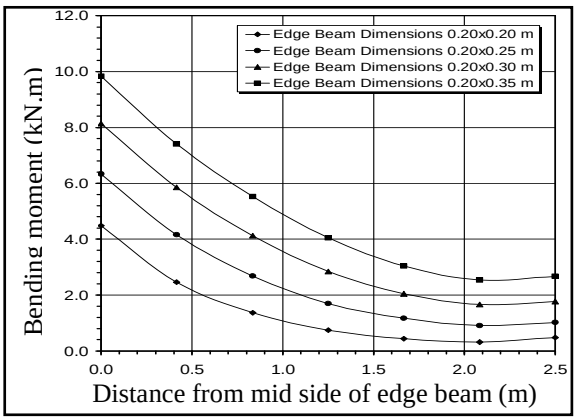


Figure 17: Edge beam bending moment variation

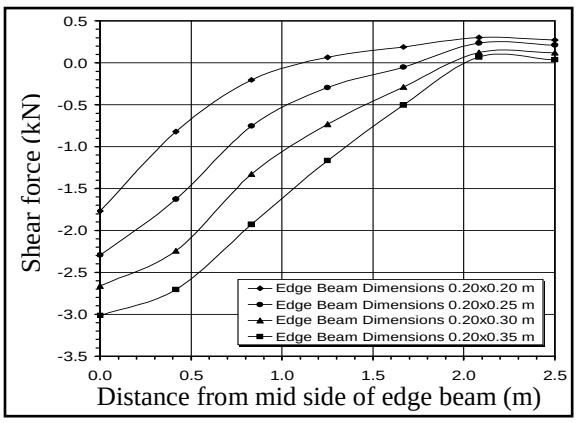


Figure 18: Edge beam shear force variation

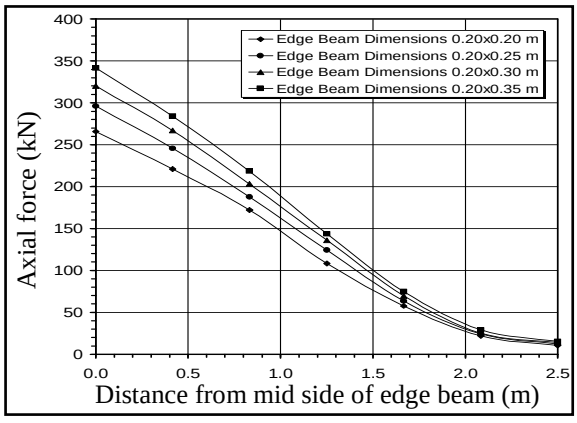


Figure 19: Edge beam axial force variation

## REFERENCES


Bairagi, N. K. & Buragohain, D.N. 1985. Application of finite element to hypar shell footings. Proc. of the 2nd International Conference on Computer Aided Analysis and Design in Civil Engineering. III: 61-69. Roorkee.

Haut, B. B. & Mohammed, T. A. 2006. Finite element stydy using FE code (PLAXIS) on the geotechnical behavior of shell footings. Journal of Computer Science 2(1): 104-108. Science Publications.

Haut, B. B., Mohammed, T. A., Abang Ali, A. A. & Abdullah, A. A. 2007. Numerical and field study on triangular shell footing for low rise building. International Journal of Engineering and Technology 4(2): 194-204.

Huang, H. C. 1989. Static and dynamic analysis of plates and shells. Springer-Verlag. London. UK.

Jain, V. K., Nayak, G. C. & Jain, O. P. 1977. General behaviour of conical shell foundations. Proceedings of the International Symposium on Soil-Structure Interaction II: 53-61. Roorkee.

Kurian, N. P. 1977. Flexure of a hypar shell on elastic foundation. Proceedings of the International Symposium on Soil-Structure Interaction I: 295-298. Roorkee.

Kurian, N. P. 1982. Modern foundations: Introduction to advanced techniques. Tata-MacGraw Hill, New Delhi.

Kurian, N. P. 1993. Performance of shell foundation on soft soil. Proceedings of the International Conference on Soft Soil Engineering. Guangzhou. 383-392.

Kurian, N. P. 1994. Behavior of shell foundations under subsidence of core soil. Proceedings XIII of the International Conference on Soil Mechanics and Foundation Engineering 2: 591-594. New Delhi

Kurian, N. P. 1995. Parametric studies on the behavior of conical shell foundations. Proceedings V East Asia-Pacific Conference on Structural Engineering and Construction II: 1733-1738. Australia.

Maharaj, K. D. 2003. Finite element analysis of conical shell foundation. Birla Institute of Technology and Science. Pilani, Rajasthan. India.

Melerski, E. 1986. Numerical Analysis of Hyperbolic Paraboloid Shell. Proceedings of the 10th Australian Conference on the Mechanics of Structures and Materials.107-112. Adelaide.

Ramiah, B. K., Purushothamaraj, P., Chichangappa, L. S. & Pinto Adrian, R. 1977. Experimental studies on shell foundations. Proceedings of the International Symposium on Soil-Structure Interaction. 299-306. Roorkee.

Scott, R. F. 1981. Foundation analysis. Prentice-Hall Inc., Englewood Cliffs. New Jersey.